An empirical-stochastic, event-based program for simulating inflow from a tributary network: Framework and application to the Sacramento River basin, California

Michael Bliss Singer and Thomas Dunne

Donald Bren School of Environmental Science and Management, University of California, Santa Barbara, California, USA

Received 4 October 2003; revised 16 April 2004; accepted 20 May 2004; published 28 July 2004.

[1] A stochastic streamflow program was developed to simulate inflow to a large river from a network of gauged tributaries. The program uses historical streamflow data from major tributary gauges near their confluence with the main stem and combines them stochastically to represent spatial and temporal patterns in flood events. It incorporates seasonality, event basis, and correlation in flood occurrence and flood peak magnitude between basins. The program produces synchronous tributary inflow hydrographs, which when combined and routed, reproduce observed main stem hydrograph characteristics, including peak, volume, shape, duration, and timing. Verification of the program is demonstrated using daily streamflow data from primary tributary and main stem gauges in the Sacramento River basin, California. The program is applied to simulating flow at ungauged main stem locations, assessing risk in fluvial systems, and detecting bed level change. *INDEX TERMS:* 1860 Hydrology: Runoff and streamflow; 1821 Hydrology: Floods; 1833 Hydrology: Hydroclimatology; 1869 Hydrology: Stochastic processes; *KEYWORDS:* flow routing, Monte Carlo modeling, Sacramento River basin, streamflow simulation

Citation: Singer, M. B., and T. Dunne (2004), An empirical-stochastic, event-based program for simulating inflow from a tributary network: Framework and application to the Sacramento River basin, California, *Water Resour. Res.*, *40*, W07506, doi:10.1029/2003WR002725.

1. Introduction

[2] For a number of purposes (estimation of flood risk, sediment transport and routing, prediction of inundation regimes of floodplain vegetation, and effects of flow regulation on all of the above) it would be useful to know about the probability distributions of flood hydrograph characteristics, including their peak, volume, shape, duration, and timing. It would also be useful to analyze these aspects of flood hydrographs on large rivers at locations other than major main stem gauging stations and to examine the effects of certain engineering modifications on flood characteristics. The commonly used flood frequency curve, derived from the annual maximum series of a single realization of one *n*-year peak flow series, does not yield as much information as could be gleaned from treating the empirical record as a sample of all other possible realizations. We propose to view the flood record in this latter fashion to derive from it some of the flood regime characteristics useful for multiple purposes, including traditional design needs in flood control and zoning as well as research and management needs relevant to ecosystem functions.

[3] There is currently a separation of responsibilities for the analysis of floods in lowland river systems. Some hydrologists are concerned mainly with floods as hazards that need to be designed for, and others view floods as agents of ecosystem maintenance that are essential for aquatic and riparian biodiversity [*National Research Council*, 2001]. Flood control engineers and planners are generally interested in large flood peaks to assess flood risk and design flood control [*U.S. Army Corps of Engineers*, 1992]. Ecologists and geomorphologists are interested in a range of floods, including those below the zero-damage stage, that transport sediments of differing caliber, inundate and scour floodplains, and maintain riparian plant communities [*Junk et al.*, 1989; *Church and Hassan*, 1992; *Poff et al.*, 1997; *McLean et al.*, 1999; *Tockner et al.*, 2000]. The two groups have different sets of methods for analyzing floods [cf. *National Research Council*, 1988; *Richter et al.*, 1996]. Therefore there is use for a single program that treats the spectrum of floods, from instantaneous flood peaks used in flood control design to hydrograph characteristics (e.g., shape and duration) that affect riparian and aquatic ecosystems [*Richards et al.*, 2002]. Such a program would simulate sequences of floods as long-term hydrographs that could be analyzed statistically or used as input to a variety of other models. The word ''flood'' is used to here to describe the large, damaging peaks that flood control systems are designed to convey and the time series of discrete flow events slightly above and below bank-full discharge.

[4] In section 2 we develop the framework of a program for simulating the statistical properties of the full range of flow hydrographs that affect flood control, the sediment transport budget, and various riparian processes. In section 3 we apply this program to the Sacramento River basin in California to verify its predictive capability, and we discuss its application in (1) simulating flow at ungauged

0043-1397/04/2003WR002725$09.00

main stem locations, (2) assessing risk in fluvial systems, and (3) detecting bed level change.

2. Framework

2.1. Background

2.1.1. Previous Work on Streamflow Simulation

[5] Streamflow simulation is the generation of synthetic discharge data over a regular time interval (e.g., days) in a river basin for use in long-range planning and development [*Fiering*, 1967]. Methods of simulating streamflow vary depending on the quantity and quality of empirical data available for a particular basin in both time and space. The two groups of these methods are (1) those that model the hydrologic processes by which rainfall becomes streamflow (hereafter called process based) and (2) those that model streamflow based entirely on historical data sets of streamflow (hereafter called empirical).

[6] Process-based methods tend to be applied in small river basins where flow data are sparse and tend to use rainfall-runoff models to simulate streamflow (see *Beven* [2000] for a discussion of the differences in data-based versus physically based rainfall-runoff models). Process-based streamflow simulations in large river basins have combined rainfall-runoff models for subbasins [*Burnash et al.*, 1973] and have linked surface properties to climate models via soil-vegetation-atmosphere transfer methods [*Nijssen and Lettenmaier*, 1997].

[7] Empirical methods tend to be applied in river basins that have been subjected to intensive data collection campaigns and attempt to preserve the statistical properties of the historical data when simulating data at a particular gauge. For example, mean annual flow should be approximately the same for observed and simulated data. However, the spatial structure and timing of flow delivery from a network of gauging stations to the main stem have been largely ignored. If these factors were incorporated into a streamflow simulation program on the basin scale, one could predict the statistical structure of main stem hydrology based on the spatial and temporal patterns of inflow from its tributaries, including the effects of flow management on tributaries. The program could be used to simulate hydrographs at any main stem location by routing simulated tributary inflows through the main channel by standard procedures [e.g., *Brunner and Bonner*, 1994].

[8] In this study we develop an empirical-stochastic program (hereafter referred to as HYDROCARLO) for simulating synchronous, event-based streamflow from major tributaries in river basins where flood control and water supply concerns have dictated long and spatially extensive streamflow gauging programs.

2.1.2. Program Strategy

[9] Spatial and temporal variability of inflow from major tributaries is the principal control on stream discharge in large river channels. Such variability results largely from rainstorm magnitude, duration, and trajectory, from rates of snowmelt, and from differential rates in runoff generation based on tributary basin characteristics (e.g., slope, elevation, and vegetation). Our goal is to simulate streamflow from a basin-wide network of tributaries as sequences of flood events by preserving seasonal oscillations in flow magnitude, flow duration, interstorm period duration, and the synchronicity in flood occurrence and flood peak magnitude, as they are reflected in historical records. The stochastic flow program would yield an infinite number of realistic simulations in the form of synchronous hydrographs from the tributary gauging network, which could be combined or routed to produce main stem hydrographs that are based on plausible patterns of tributary inflow.

[10] The empirical approach to streamflow simulation presented here is not concerned with understanding the complexities of streamflow generation (i.e., how rainfall is converted to runoff and routed through a network). Instead, the program we demonstrate herein focuses on stochastic simulations of streamflow based on relationships between tributary streamflow records. Consequently, our approach cannot account for nonstationarities (which may be explicitly represented in a hydrologic response model) in basin conditions such as surface properties (e.g., deforestation) or reservoir operation unless the timing of these influences is known a priori.

2.2. Stochastic Approach

[11] We conceptualize an idealized large river basin as a main stem with (say) six major tributaries, each of which has a streamflow gauge near the confluence (Figure 1). The main channel has a gauge (labeled 0 in Figure 1) to monitor streamflow entering the reach from upstream and a gauge to monitor streamflow at the basin outlet. Each gauge has recorded mean daily streamflow for 50 years.

[12] A purely empirical approach to streamflow simulation would route contemporaneous measured inflow from all tributary gauging stations in the network through the main channel to reproduce the 50 years of historical record at the basin outlet. This deterministic modeling strategy allows for only one outcome based on the historical record and does not represent the variable nature of flow delivery to the main channel. Following the recommendations of other researchers [e.g., *Hirschboeck*, 1988, pp. 39–42], we have opted for a stochastic approach to modeling tributary inflow in order to represent the potential variability in (and thus the uncertainty in predicting) storm magnitude, frequency, duration, trajectory, snowpack, melt rate, and tributary basin characteristics and condition.

[13] The theory of stochastic processes acknowledges that some physical processes cannot be modeled accurately on the basis of available data and existing theories, rooted in first principles. The theory instead relies on the use of probability to represent uncertainties in the theory. Stochastic modeling of hydrologic data extends back at least as far as the application of creating longer streamflow series by sampling at random from annual historical series for a given location [*Sudler*, 1927]. Its methods later became more formalized using statistical theories to develop autoregressive models for monthly rainfall data [*Hannan*, 1955]. Since that time, stochastic statistical theory has been applied to empirical streamflow simulation primarily to synthetically extend the historical record of annual maximum series at a particular gauging point [e.g., *Stedinger and Taylor*, 1982] and to generate synthetic series for ungauged basins using regional parameters [e.g., *Benson and Matalas*, 1967].

[14] We use HYDROCARLO as a stochastic seasonal flood generator at a network of streamflow gauging points. Each gauge can be thought of as a valve that is opened when a flood occurs (solid arrows in Figure 1). During interstorm

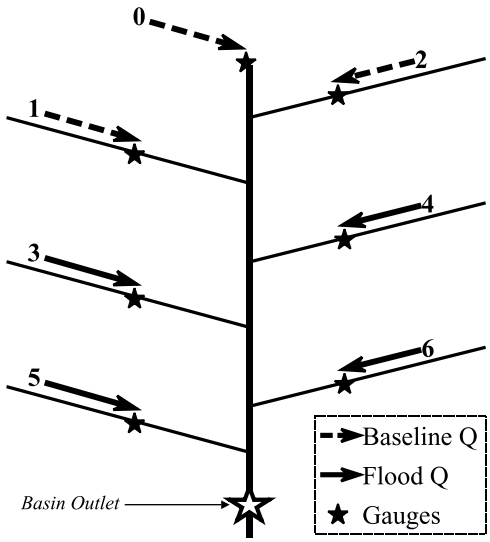

Figure 1. An idealized depiction of a drainage basin with a network of tributary gauges. Figure 1 shows one example of a range of possible rainstorms. In this case, the winter frontal rainstorm is inducing flood conditions at gauges 3–6, while gauges 0–2 are unaffected.

periods the valve at a gauging station never closes completely but instead "leaks" with a flow magnitude equivalent to the base flow discharge (dashed arrows in Figure 1). There are numerous combinations of uncertain variables (e.g., rainstorm trajectory and tributary basin condition) that could induce flood conditions at some gauges while leaving others unaffected. Figure 1 illustrates the effect of a seasonal storm (e.g., a frontal rainstorm in winter) on a trajectory through the southern portion of the idealized basin, inducing flood conditions at gauges 3, 4, 5, and 6 but leaving gauges 0, 1, and 2 unaffected. In the development of HYDROCARLO we have accounted for the numerous possible combinations of season, storm characteristics, and drainage basin conditions that could affect streamflow at all tributary gauges in a basin. Lacking the data or understanding to model these factors explicitly, we represent them in HYDROCARLO by stochastically drawing upon historical flood data from tributary gauges, which reflect seasonal storm patterns, the frequency of storms at each gauge, and the correlation in storm conditions between gauges.

2.3. Program Initialization

[15] HYDROCARLO's fundamental features are (1) seasonality, (2) representation of flood events, and (3) basin-wide synchronicity. Each will be discussed separately in terms of program initialization (Figure 2).

2.3.1. Seasonality

[16] Seasonal controls on discharge differ by geographic region, and these differences are detectable in annual hydrographs. For example, in some river basins, discharge hydrographs are influenced by large frontal rainstorms in the winter (e.g., Sacramento River in California). Others receive the majority of their precipitation from a summer monsoon (e.g., Narmada River in India). The predominant flood pulses of other basins result from the melting of snow and glaciers in the spring (e.g., Copper River in Alaska). Distinct seasonal flood hydrographs are produced in each climatic setting [*Hirschboeck*, 1988]. In addition to seasonally varying flood peak magnitude, there are seasonal controls on the probability of flood event occurrence (e.g., floods are less frequent in a dry season), the length of interstorm periods, and the magnitude of base flow.

[17] We parameterize these seasonal discharge attributes in HYDROCARLO with user-defined seasons for a given set of input data. The program uses the seasonal definitions to separate flood events and to calculate event probability and base flow magnitude. For example, a flow series with wet winters and dry summers would be separated into two hydrologic series from which flood events would be extracted and stored in matrices (Figures 2 and 3). The flood event probability and base flow discharge would also be calculated for each season, according to a procedure described in section 2.3.2.

2.3.2. Event Basis

[18] Our intention is to simulate decades-long hydrographs at tributary gauging points using combinations

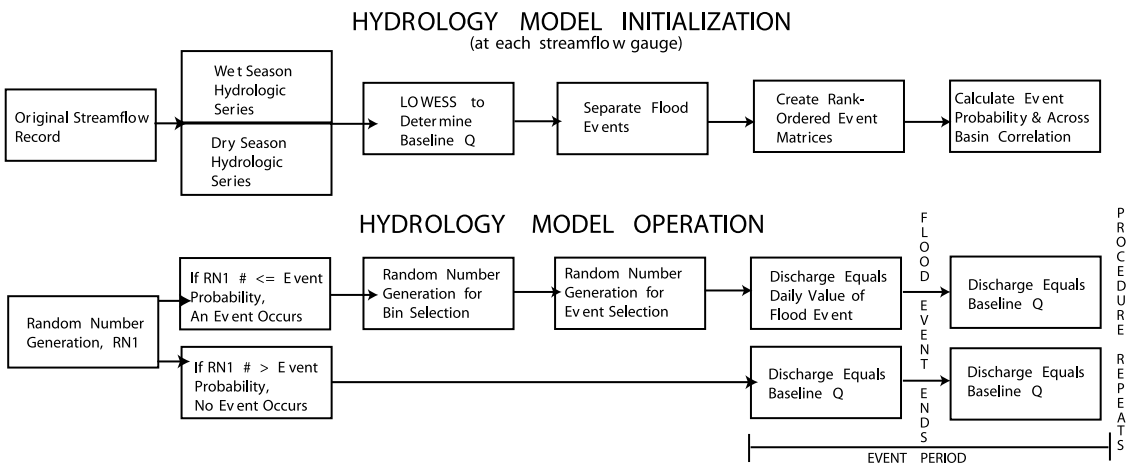

Figure 2. Flowchart showing important steps in model initialization which occur at each gauge and model operation which occurs for all gauges simultaneously. RN1 (in model operation) corresponds to the random number generated at the beginning of each event period and is compared to the event probability at all gauges.

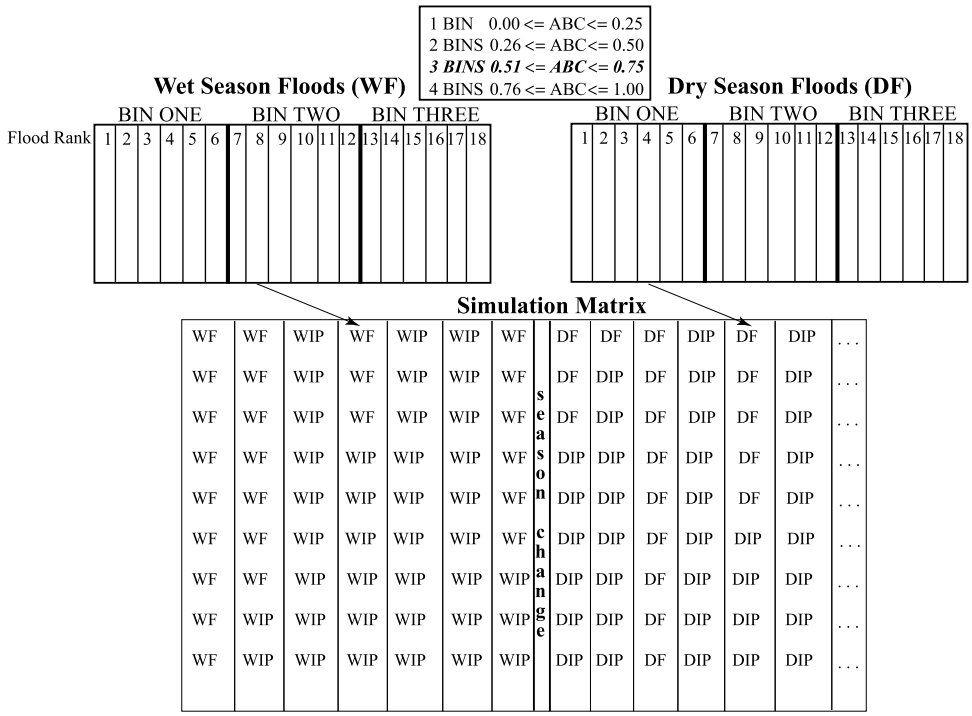

Figure 3. Diagram describing assemblage of the simulation matrix (center) at each tributary gauge. In initialization, floods (sequences of flood discharge days) are placed into each flood matrix in peak rank order. Across-basin correlation (ABC) is calculated to determine the number of bins for dividing flood matrices. In this idealized case, ABC = 0.72, and each flood matrix is divided into three bins (top). In operation, one random number is generated and compared to event probability at each gauge in the basin in each event period to determine whether an event occurs. Then a bin number is chosen at random. Another random number is generated separately at each gauge with an event to select a specific flood from within the chosen bin. Each column represents an event, which includes a column of discharge days with length equal to the event duration. Hence the first two columns of the depicted simulation matrix contain wet season floods (WF) of 9 and 7 days, corresponding to two consecutive event periods. For simplification, all depicted event periods are 9 days long (i.e., each column has nine rows). If no flood is selected for a given event period (see text), the column is comprised of seasonal interstorm or baseline discharge days (e.g., WIP for wet season interstorm periods) of duration equal to the event period (e.g., third column). Likewise, WIP is used when the selected flood terminates before the end of the event period (e.g., second column). The program switches between seasons based on the number of days determined for a given season. This continues for the duration of the simulation.

of recorded flood events from the historical flow record at each gauge (i.e., sequences of discharge days above a threshold value). We call this threshold the baseline discharge and obtain it using the locally weighted scatterplot smoothing (LOWESS) procedure [*Cleveland*, 1979]. LOWESS is essentially a moving average, which discounts the influence of points that deviate dramatically from the previous smoothed value. We use LOWESS to obtain a smoothed curve for each seasonal hydrologic series at each gauge and then calculate the mean of that curve and call it baseline discharge (Figures 2 and 4). Figure 4 shows a collection of wet season events that have been patched together to calculate the baseline discharge. We ignore the magnitude of flows below the baseline discharge because they are insignificant to sediment transport, flood dike stability, and most aspects of river restoration, although this baseline could be lowered for investigations of low-flow conditions.

[19] After determining the baseline discharge for each seasonal flow series, we discretize continuous sequences of flood days (i.e., those above the baseline discharge) into flood events of varying magnitude and duration (Figure 4). We store each historic flood event as a column vector in a flood event matrix (Figure 3) in rank order of flood peak magnitude. We define event probability for each flow series at each gauging station by dividing the number of days in the partial duration flood series (i.e., those above the baseline discharge) by the total number of days in the flow record. This measure is essentially the probability of a flood day, which is distinctly different from the number of floods per unit time. However, in our program's operation, a realistic number of flood days is simulated at each gauge because HYDROCARLO operates per event period by simulating synchronous floods of differing durations at each gauge (see below).

[20] In addition to the flood event matrix for each gauge a matrix of interstorm periods is generated at the gauge with the longest record. This matrix is seasonally composed of interstorm period lengths (i.e., sequences of days below the seasonal baseline discharge) which represent the range of

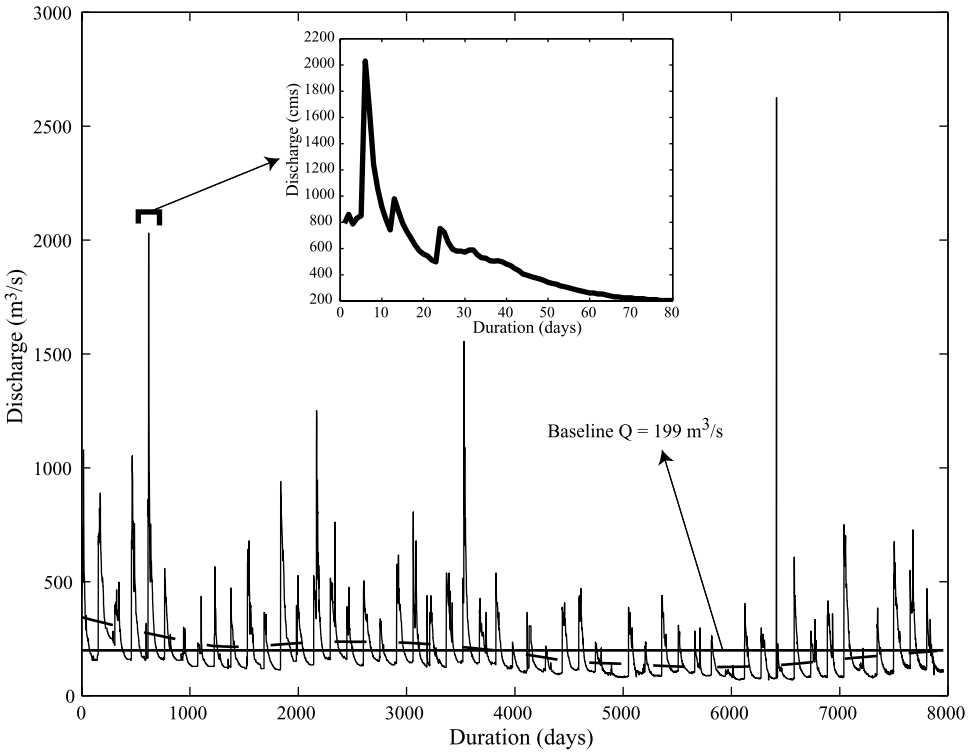

Figure 4. An example of baseline discharge calculation for the dry season flood series from Bend Bridge on the Sacramento River. The plot consists of a patchwork of all flood days in the dry season over a 49-year period. A smooth LOWESS curve is first fitted to the data (dashed line) and then its mean is calculated and called the baseline Q (labeled). Baseline Q is the threshold for a flood event. Discharge days above the threshold are considered flood days and those below the threshold are considered interstorm periods. Baseline Q is calculated separately for each seasonal series. Inset shows how individual flood events are separated using the baseline Q.

basin-wide interarrival times that could occur in the basin over the long term.

2.3.3. Correlation in Events

[21] There is no continuous field of streamflow as a function of distance between two nearby gauges on distinct tributaries, as can be assumed for rainfall in point process models [e.g., *Rodriguez-Iturbe et al.*, 1987], because each streamflow gauge makes measurements of flow that is fed through a discrete tributary basin. However, nearby tributary basins that have similar characteristics (e.g., drainage area, slope, land use, and vegetation) are likely to produce similar synchronous streamflow near their confluences with the main channel if there are no orographic effects that consistently cause more rainfall to occur in one basin over the other. However, there are conceptual problems with developing a program that represents this type of relationship as something other than totally similar or totally random. For this purpose we combine a stochastic approach with empiricism based on historical flood records.

[22] In HYDROCARLO we represent two types of spatial and temporal correlation in flood events between gauges. First, we account for correlation in flood event occurrence via the event probability at each gauge. This correlation arises because two gauges located in close proximity are likely to have flood conditions induced by the same storms in a particular season and a similar number of flood days and thus similar seasonal event probabilities. Conversely, gauges farthest from each other are likely to have different seasonal event probabilities because prevailing storm trajectories may favor rainfall in one tributary basin over another. For example, Figure 1 illustrates a southerly storm trajectory that might consistently cause rainfall in the tributary basin of gauge 5 and consistently cause low rainfall in the basin of gauge 2. One could imagine orographic and other localized effects that could induce similar conditions. These effects would be reflected in the number of flood days and thus the event probabilities for each season at these stations (hereafter referred to as seasonal event probabilities).

[23] Second, we account for correlation in flood peak magnitude between gauges for synchronous flood events (i.e., events that are measured at two or more gauges on the same day). This correlation arises from regional storm cells that generate consistent spatial patterns of rainfall over a basin. These patterns, in turn, induce flood peaks of similar rank order at each gauge, whether or not these peaks occur simultaneously at each gauge. Thus we expect synchronous floods at nearby gauging stations to have similar flood event ranks (i.e., of relative magnitude). For example, if the winter frontal storm in Figure 1 caused the tenth magnitude event (column 10 in the wet season flood matrix in Figure 3) at gauge 3, it is reasonable to assume that gauge 5 would have an event ranking similar but not necessarily equal to 10. We sought to maintain this spatial correlation in flood peak ranking in HYDROCARLO while retaining the maximum amount of randomness in event selection. Therefore we

assess correlation in all flood peaks (i.e., not only annual maxima) from synchronous events recorded at gauges at opposite ends of a river basin. HYDROCARLO stores the flood peaks from these events at each gauge and calculates the cross correlation between their peak discharges, which we call the across-basin correlation (ABC), calculated as

$$\mathrm{ABC}_{05} = \frac{\gamma_{05}}{\sigma_0 \sigma_5}, \quad (1)$$

where γ_{05} is the covariance in synchronous flood peaks between gauges 0 and 5 (Figure 1), for example, and σ_0 and σ_5 are the standard deviations in flood peaks at gauges 0 and 5, respectively. We calculate ABC specifically for widely separated gauges in order to characterize the spatial correlation for the basin as a whole according to the presumed least correlated gauges in the network.

[24] We use ABC to develop a system of relative flood selection in HYDROCARLO. We divide the ranked column vectors in seasonal flood event matrices (Figure 3) into a number of bins that is determined according to ABC (Figure 3). To illustrate the process of relative flood selection, suppose there were 18 flood events (i.e., 18 column vectors) in the wet season flood event matrix for each gauge in the idealized basin (Figure 1), and the ABC (i.e., between gauges 0 and 5) was 0.72. The seasonal flood matrix for each gauge in the basin would be divided into three bins, each containing six flood events (Figure 3).

[25] The number of bins into which floods are divided indicates the degree to which flood event magnitude is related for gauges in the basin. If the flood series for each gauge in a basin were divided into four bins (high ABC), there would be a high probability that selected floods at each gauge will be of similar relative magnitude at any particular time step. Conversely, if floods in a basin were lumped into one bin (low ABC), there would be a low probability that selected floods at each gauge would be of similar relative magnitude at any particular time step. The bins represent a narrowing of the flood event selection pool according to the influence of basin-wide storms. Generally, river basins with higher across-basin correlation are likely to be small, homogenous (in topography and vegetation), or commonly affected by basin-wide storms or snowmelt. River basins with lower across-basin correlation would include those that are very large or heterogeneous or that have a number of climatic zones accessed by different tributaries.

2.4. Program Operation

[26] Random numbers are generated in HYDROCARLO to determine flood occurrence at each gauge and to select flood events from each gauge, when they occur. All random numbers are generated using MATLAB's rand function, which generates pseudorandom numbers by consistently resetting the generator to its initial state. Flood events and interstorm periods are simulated in the various seasons and stored in a simulation matrix for each gauge (Figure 3). Reference to Figure 2 may clarify the following detailed discussion of program operation.

[27] HYDROCARLO first generates a random number between 0 and 1 (RN1 in Figure 2) and compares it to the seasonal event probability for each gauge (i.e., the probability that a flood will occur on any particular day of that season). If RN1 is greater than a gauge's seasonal event probability, then no event will occur at the gauge. If RN1 is less than or equal to the seasonal event probability, an event will occur at this gauge. We acknowledge that this procedure does not explicitly account for the structure of cross correlation in flood occurrence between gauges but is reasonable for simulating heterogeneous occurrence in basins affected by basin-wide rainstorms. HYDROCARLO then randomly selects one bin out of the bin structure specified by the ABC, from which all synchronous floods will be chosen. The program generates another random number (an integer between 1 and the number of event columns in that bin) to select flood events at each gauge (i.e., each gauge where a synchronous event occurs). For example, assuming the ABC were 0.72 for the idealized basin at the depicted point in time (Figure 1), if bin 2 were selected randomly, then flood events at gauges 3, 4, 5, and 6 would be selected at random from event ranks 7–12 of their respective flood event matrices (Figure 3).

[28] The historical daily streamflow for the selected event at each gauge is then entered into the simulation matrix as a column vector (like Figure 3). In this empirical-stochastic approach, there may be multiple events of varying duration occurring at different gauges simultaneously. We have defined the length of an event period as the duration (in days) of the longest event selected for that period. Therefore, when an event for a gauge terminates before the end of the event period, HYDROCARLO resets the discharge for that gauge to the seasonal baseline discharge until the end of the event period (i.e., until the longest flood event among the tributaries is complete). Similarly if no event occurs at a particular gauge for an event period, the appropriate column in its simulation matrix will contain seasonal baseline discharge for the duration of the event period (Figure 3). Discharge at any gauge never falls below its seasonal baseline discharge. At the completion of the event period, HYDROCARLO generates a new RN1 to compare with event probabilities at all gauges and the selection procedure repeats (Figure 2). HYDROCARLO creates a new column in the simulation matrix for each event period.

[29] If no event is selected at any gauge for an event period (i.e., RN1 is greater than the event probability at all gauges), HYDROCARLO selects a basin-wide interstorm period duration by randomly choosing a column from the seasonal matrix of interstorm periods discussed in section 2.3.2. In simulation the program assembles in each gauge's simulation matrix a column of interstorm days with length equal to the duration of the selected interstorm period and with values equal to the seasonal baseline discharge for that gauge.

[30] As the program proceeds through event periods, the simulation matrix at each gauge grows with the selection of flood events punctuated by interstorm periods in alternating user-defined seasons (Figure 3). Because of its employment in a stochastic program, the user definition of season length is not followed exactly. For example, if there are 10 days remaining in the wet season and an 11-day flood event is selected from the wet season flood matrix, this event will complete its 11-day progression before the program switches to the dry season matrix for flood selection. Once a simulation is complete, the simulation matrix assembled at

each gauging point can be concatenated to form a hydrograph with length equal to that of the simulation.

3. Program Application

3.1. Basis for Application

[31] There are two purposes to this part of the paper. First, we validate the capability of HYDROCARLO to simulate hydrographs on the main stem Sacramento River in California, using mean daily streamflow data from the U.S. Geological Survey (USGS) for primary Sacramento tributaries. We (1) simulate the sequence of inflow at primary tributary junctions, (2) route simulated tributary inflow through the main stem Sacramento, (3) construct probability distributions of flow characteristics from simulated, main stem hydrographs, and (4) compare these distributions with probability distributions derived from independent historical data for the same locations. Second, we discuss how HYDROCARLO can be applied for practical purposes in other multiple-use river basins.

[32] There have been several quantitative streamflow studies in the Sacramento River Basin. Previous work has mostly focused on evaluating the sensitivity of streamflow to climate change. This has been accomplished empirically by relating streamflow to temperature [*Risbey and Entekhabi*, 1996] and by predicting monthly and seasonal runoff with the aid of a water balance model [*Gleick*, 1987]. Process-based methods have been used in the Sacramento to model runoff using temperature estimates from general circulation models in medium-sized test basins [*Lettenmaier and Gan*, 1990] and to evaluate the impact of warming on the State Water Project [*Lettenmaier and Sheer*, 1991]. Other studies have aimed to extend historical streamflow records on the Sacramento over millennial timescales using isotopic analysis on fossil bivalves [*Ingram et al.*, 1996] and to investigate climatic changes over centuries using tree ring analysis [*Earle and Gritts*, 1986].

[33] One area of study absent from this list involves fully utilizing the abundant streamflow data set available for the Sacramento River basin within a streamflow simulation program that represents recent hydroclimatology as spatial and temporal patterns of daily tributary inflow to the main stem. We fill this void by applying HYDROCARLO to the Sacramento data to simulate the range of potential flood events that could occur in the basin. To reiterate, we use the word "flood" here to describe not only the largest peaks that flood control systems are designed to convey but also the time series of discrete high-flow events slightly above and below bank-full discharge. We are simulating complete floods that are relevant to flood control engineers, ecologists, and geomorphologists.

3.2. Sacramento River Basin

3.2.1. Geographical Background

[34] The Sacramento River drains the northern part of the Central Valley of California and has a total drainage area of 6.8×10^4 km^2 comprising over one half of the total drainage area into San Francisco Bay. It flows from its source near Mount Shasta 600 km south to its confluence with the San Joaquin River, where the two rivers form the San Francisco Bay Delta. The Sacramento flows for ~400 km within its low gradient valley (mean slope ~0.0002). Its tributaries rise from the Coast Ranges in the west, the Trinity Mountains in the northwest, the Modoc Plateau in the northeast, and the Sierra Nevada in the east.

[35] The Sacramento is a rare large river in that its channel capacity gradually decreases in the downstream direction between the historic Butte Creek and Feather River confluences (Figure 5), leading prehistorically to extensive floodplain inundation [*Gilbert*, 1917; *Kelley*, 1998]. The advent of permanent human settlement into this flood regime led to the Sacramento Valley Flood Control Project, a system of flood control levees, weirs, and bypasses built between 1917 and 1933 [*Water Engineering and Technology*, 1990], designed to convey flood waters through the Sacramento River and adjacent floodways. To relieve pressure on the channel banks, high flows are diverted into Sutter and Yolo Bypasses via five major weirs. The flood control system was bolstered between 1943 and 1970 with the construction of a number of dams. Major dams include Shasta Dam (capacity 5.6×10^9 m^3) upstream of Keswick on the Sacramento River, Oroville Dam (capacity 4.4×10^9 m^3) on the Feather River, Folsom Dam (capacity 1.2×10^9 m^3) on the American River, and Whiskeytown Dam (capacity 3.0×10^8 m^3) on Clear Creek (Figure 5). These dams are operated for various combinations of flood control, hydroelectricity, water supply, irrigation, and recreation (data are from the U.S. Bureau of Reclamation dam selection Web site, http://www.usbr.gov/dataweb/dams).

3.2.2. Sacramento Hydroclimatology

[36] The Sacramento Valley has a Mediterranean climate with mostly dry summers and wet winters dominated by large frontal rainstorms in the winter with occasional snowmelt floods in the spring. Annual precipitation in the basin ranges from 25 cm in the southern part of the valley to 250 cm in the mountains to the north and east with >80% of precipitation occurring between November and March [*Jones et al.*, 1972]. The majority of the flood flow at the basin outlet originates in the mountainous portions of tributary basins and not in the Sacramento lowland [*Thompson*, 1960]. Moderate-sized floods can be generated from melting snowpack in the Sierra Nevada, but major floods in the Sacramento River under present conditions of flood control are generated by rain on melting snow during winter [*Thompson*, 1960]. Many tributaries flow into the Sacramento (Figure 5), including the large American and Feather Rivers that drain the Sierra Nevada. Discharge contribution from Coast Range tributaries is limited because they have drier climates, and many are controlled by impoundments or captured by a system of irrigation canals that run parallel to the Sacramento River. The northern perennial streams rise from the Trinity Mountains to the northwest and the Modoc Plateau to the northeast.

[37] We applied HYDROCARLO to the main stem Sacramento River south from Keswick (below Shasta Dam) to the town of Freeport (south of the city of Sacramento), using data from primary tributaries near their confluence with the main stem (Figure 5). We define primary tributaries in this basin as those which have drainage areas of at least 300 km^2 and at least 10 years of continuous daily streamflow data. Our drainage area threshold of 300 km^2 is approximately 0.5–1% of the total drainage area for the study area (5.2×10^4 km^2). The total study area was calculated by subtracting drainage area disconnected from

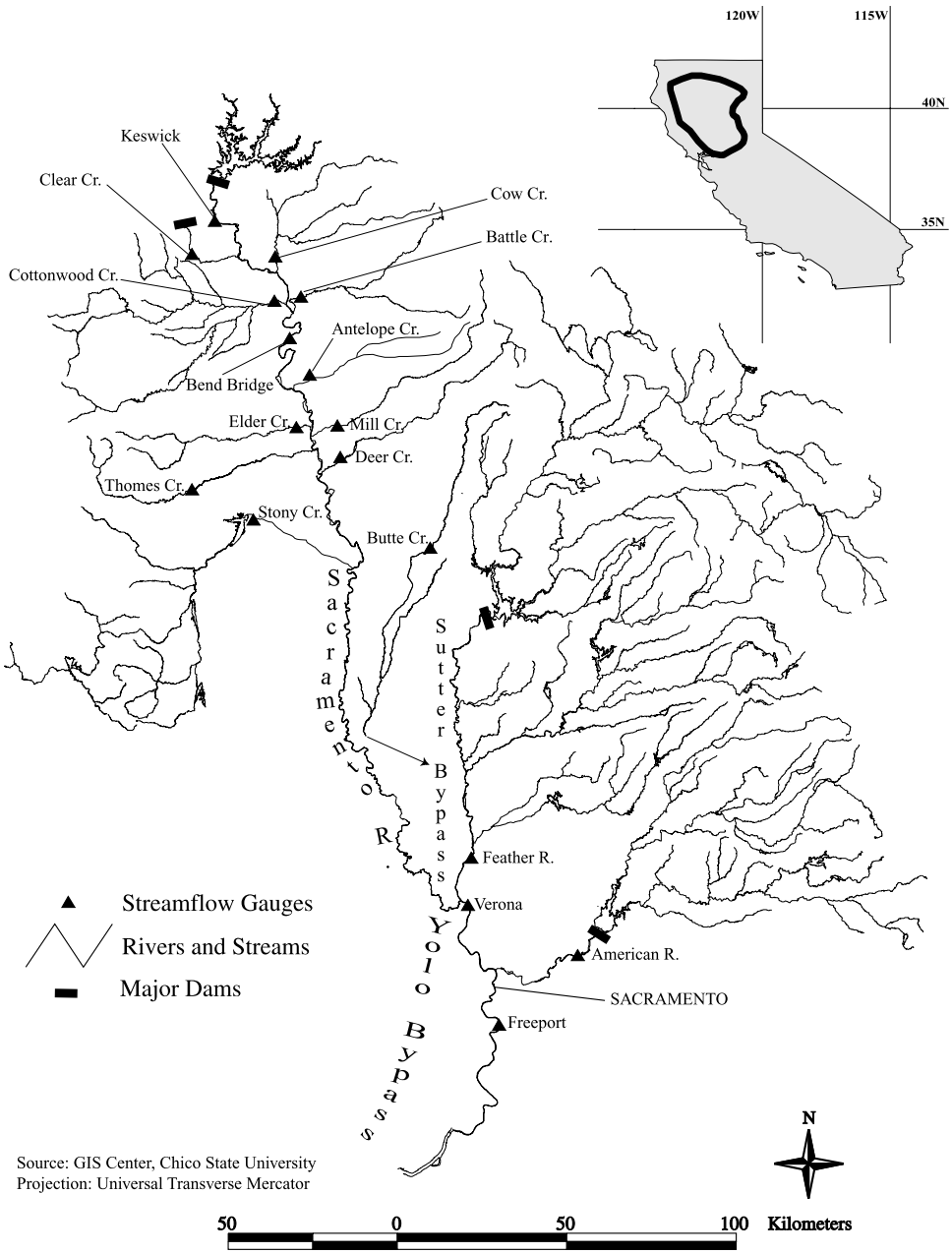

Figure 5. Map of Sacramento River drainage basin showing primary tributaries, gauges, flood bypasses, and major dams. Flood diversion weirs are not depicted. Note that Butte Creek does not actually join the Sacramento but instead drains into a slough, which flows east directly into Sutter Bypass. Sutter Bypass flows south, where it ultimately joins the Sacramento River at the Feather River confluence. Combined flows from main stem Sacramento River, Feather River, and Sutter Bypass periodically overtop Fremont Weir and flow into Yolo Bypass to the delta.

the main stem Sacramento by engineering structures from the drainage area at Freeport. The majority of daily flow records from Sacramento tributaries span several decades, so we have chosen 10 years as a timescale representative of the hydroclimatological correlation in flow records between gauges. Therefore we used only flow records from stations that had records of at least 10 years. Two creeks that fit our drainage area criterion, Pine Creek (536 km^2) and Burch Creek (412 km^2), were omitted from this analysis because of lack of streamflow records.

[38] Figure 5 shows the primary tributaries and the gauges used in this study for historical flood selection, and Table 1 shows statistics on each primary tributary. The primary tributaries used in this study comprise more than 90% of the study area. We included additional tributaries in our HYDROCARLO simulations to account for the ungauged drainage area. Below we discuss the specifics of which tributaries were selected for each simulation period and how they were built into flow routing.

3.3. Regional Parameterization

[39] Regional parameterizations of seasonality, event basis, and correlation in events are outlined below. However, we make an additional modification to hydrologic data

Table 1. Tributary Basin Characteristics[a]

Basin Name	USGS Station	DA, km^2	Years of Q Data	Mean Q	Maximum Q	Dam
American River	11446500	5014	1904–1997	106	3738	X
Antelope Creek	11379000	319	1940–1982	1	161	
Battle Creek	11376550	925	1940–1996	14	309	
Sacamento River at Bend Bridge	11377100	23051	1891–1999	340	7392	X
Butte Creek	11390000	380	1930–1999	12	753	
Clear Creek	11372000	591	1940–1999	8	428	X
Cottonwood Creek	11376000	2401	1940–1999	25	1538	
Cow Creek	11374000	1101	1949–1999	20	920	
Deer Creek	11383500	544	1920–1999	9	569	
Elder Creek	11380500	352	1949–1969	3	237	
Feather River	11425000	15335	1943–1983	245	8863	X
Sacamento River at Keswick	11370500	16752	1938–1999	267	4531	X
Mill Creek	11381500	339	1928–2000	9	408	
Stony Creek	11388000	1911	1955–1990	15	680	X
Thomes Creek	11382000	526	1920–1996	8	844	

[a]The characteristics include the U.S. Geological Survey gauging station number, drainage area (DA), years of data available, the mean annual flood, the maximum mean daily flood, and the presence or absence of a major upstream dam.

sets that are influenced by major dams on the following tributaries: Sacramento River at Keswick, the Feather River, the American River, and Clear Creek. We discarded hydrologic data that were recorded during the period of reservoir filling (using information provided by the U.S. Bureau of Reclamation and the California Department of Water Resources (CDWR)), a period that was not representative of natural or regulated flow conditions. We divided the remaining data at these gauges into predam and postdam hydrologic series. Stony Creek also has upstream impoundments (Table 1), but the historical record at the gauge employed in this study was not operational in the predam era.

3.3.1. Seasonality

[40] We subdivided predam and postdam Sacramento basin hydrologic series into two flood seasons: a wet season (1 November to 31 May) and a dry season (1 June to 31 October). We considered dividing the flood record into three seasons to represent the snowmelt period in the Sierra Nevada as a separate season. We inspected plots of February-March and April-May flow data for each of 20 years recorded at Feather River in the predam era and could not detect obvious differences in the populations of flood events between them (e.g., flood duration, baseline discharge). The lack of a distinct snowmelt flood signal may be due to its attenuation over significant travel distance from the melting snow and the mixing of meltwater with rain-derived floodwater from foothill tributaries. Therefore we conservatively assume that there is no distinct hydrograph expression in the snowmelt season for Sierra tributaries and, by extension, for the Sacramento Basin as a whole, and therefore we model the basin with one wet and one dry season. We recognize the limitations of a user-defined approach to representing seasonality in our program but have not as yet developed a more rigorously objective approach. However, our approach is no less objective for defining seasons than traditional flood frequency techniques of segregating mixed flood populations by their generating mechanisms [cf. *Hirschboeck*, 1987].

3.3.2. Event Basis

[41] At each gauge we determined the baseline discharge and calculated the event probability for a season for each hydrologic series (i.e., predam wet season, postdam wet season, predam dry season, etc.) according to the procedure described in section 2. Table 2 shows the seasonal baseline discharge calculated for predam and postdam simulations at each tributary gauge.

[42] The process of defining the baseline discharge and calculating event probabilities provides some insight into the differences between wet and dry seasons in predam and postdam hydrologic regimes. For example, since dams were constructed on impounded tributaries (e.g., Feather River and American River), the baseline discharge and the event probability (i.e., the frequency of flows above baseline) at these gauges have increased in the dry season and decreased in the wet season to serve irrigation and flood control (Table 2).

3.3.3. Correlation in Events

[43] We calculated seasonal ABC for predam simulations using data from Bend Bridge and American River for 1905–1942 and for postdam simulations using data from Keswick and American River over the years 1964–1997. We used the following criteria to determine the number of bins into which the flood matrices were divided: one bin for $\rho \leq 0.25$, two bins for $0.25 < \rho < 0.50$, three bins for $0.50 < \rho < 0.75$, and four bins for $0.75 < \rho < 1.00$. The predam result is an ABC of 0.79, and the postdam result is an ABC of 0.78. High ABC for both predam and postdam series signifies that the Sacramento River Basin is affected by regional storms. This interpretation is corroborated by inspection of National Climatic Data Center historical precipitation maps (http://lwf.ncdc.noaa.gov/oa/ncdc.html) for storm days, which portray high daily rainfall totals over most of the basin.

3.4. Program Verification

[44] We checked whether simulated hydrographs (i.e., 50 n-year runs of the program) routed through the main stem are statistically similar to historical data for these locations. Verifying HYDROCARLO at a gauge located some distance downstream from tributary confluences (e.g., at the basin outlet) requires explicit flood routing to account for channel dimensions, the velocity of flowing water, overbank flow storage and losses, diversion weirs, and channel characteristics such as roughness. We used the flow

Table 2. Model Initialization Parameters[a]

Basin Name	Wet Event Probability	Dry Event Probability	Wet Baseline Q, cm s^{-1}	Dry Baseline Q, cm s^{-1}	Floods/Bin (Wet)	Floods/Bin (Dry)
Predam Simulations, ABC = 0.79						
American River	0.316	0.314	118	92	54	15
Antelope Creek	0.236	0.261	6	2	68	16
Bend Bridge	0.306	0.296	445	199	72	18
Butte Creek	0.298	0.309	15	7	88	25
Deer Creek	0.286	0.261	12	5	111	27
Elder Creek	0.258	0.219	5	0.6	30	7
Feather River	0.317	0.276	292	124	23	7
Mill Creek	0.285	0.354	10	7	134	29
Stony Creek	0.170	0.349	22	8	25	14
Thomes Creek	0.299	0.249	12	3	107	27
Postdam Simulations, ABC = 0.78						
American River	0.282	0.383	108	97	27	35
Antelope Creek	0.236	0.314	6	2	91	21
Battle Creek	0.337	0.334	17	9	125	34
Butte Creek	0.298	0.309	15	7	118	34
Clear Creek	0.171	0.213	7	2	60	24
Cottonwood Creek	0.263	0.289	38	7	88	30
Cow Creek	0.252	0.260	29	5	131	28
Deer Creek	0.286	0.261	12	5	147	36
Elder Creek	0.258	0.219	5	0.6	40	9
Feather River	0.262	0.465	283	142	11	8
Keswick	0.251	0.487	259	293	35	30
Mill Creek	0.285	0.354	10	7	179	38
Stony Creek	0.170	0.349	22	8	33	19
Thomes Creek	0.299	0.249	12	3	143	35

[a]Event probabilities (determined by baseline discharge) are higher in the dry season for many stations (especially postdam), but flood discharge in the dry season is very low and has a minimal contribution to flood frequency curves.

routing package HEC-RAS to model these factors [*Brunner and Bonner*, 1994]. The cross-sectional data for the lower Sacramento were extracted from a U.S. Army Corps of Engineers (USACE) bathymetric survey from 1997, and those for the upper Sacramento were taken from a 2001 CDWR bathymetric survey. Hydraulic roughness values for the channel and adjacent floodplain were obtained from calibrations by USACE and CDWR for their respective data sets. Locations and dimensions of diversion weirs were obtained from U.S. Geologic Survey 1:24,000 topographic maps and from CDWR.

[45] We represented the Sacramento River within HEC-RAS geometrically as a single channel with ~1000 cross sections spaced ~0.4 km apart. All flow modeling was conducted downstream of major reservoirs. Dimensions and locations of major flood diversion weirs were included in the modeling as lateral spill weirs according to standard HEC-RAS procedures [*Brunner and Bonner*, 1994]. The flow over Moulton, Colusa, and Tisdale weirs was routed into Sutter Bypass east of the Sacramento, where it was added to the tributary inflow from Butte Creek and Feather River. Flow over Fremont and Sacramento Weirs is routed to Yolo Bypass, which drains back to the Sacramento River outside of our model space. The downstream boundary condition (outside the model space) was specified as normal depth using a roughness value from USACE. Whereas each of the other weirs is operationally passive, Sacramento Weir has 48 gates that are opened and closed by the USACE and CDWR according to a complex set of rules [*U.S. Army Corps of Engineers*, 1998]. However, to simplify our HEC-RAS modeling, we represent Sacramento Weir as a passive weir with elevation equal to that at the bottom of the gates. We recognize that this may introduce consistent bias to flows routed downstream of this weir but could devise no better modeling strategy for this weir given the complexity of the flood control system.

[46] We ran HEC-RAS with unsteady lateral inflow on a daily step (with an hourly computational time step) using hydrographs stochastically generated by HYDROCARLO at each primary tributary (HEC-RAS employs an implicit finite difference solution to the one-dimensional flow equations [*Barkau*, 1997]). Lateral inflow from ungauged drainage area was represented by simulated flow from selected tributaries (named below) at locations that best approximate locations of ungauged confluences.

[47] We analyzed flood frequency statistics for the routed flows and compared them to frequency statistics for completely independent historical streamflow records at gauges near the basin outlet. In predam and postdam simulations we verified the program's ability to simulate the central tendency and distribution of the following hydrograph characteristics: (1) annual maximum flood peak, (2) mean annual flood, (3) total annual flood volume, (4) mean annual flood duration, (5) mean annual interarrival time, and (6) number of flood days. Annual peaks were calculated by selecting the maximum discharge of each year for both historical and simulated data. Mean annual flow, flood volume, flood duration, and number of flood days were calculated for the partial duration series above the wet season baseline discharge. Return periods can be computed from exceedence probabilities from any Monte Carlo model, whether or not it correctly represents the actual extreme events. This is

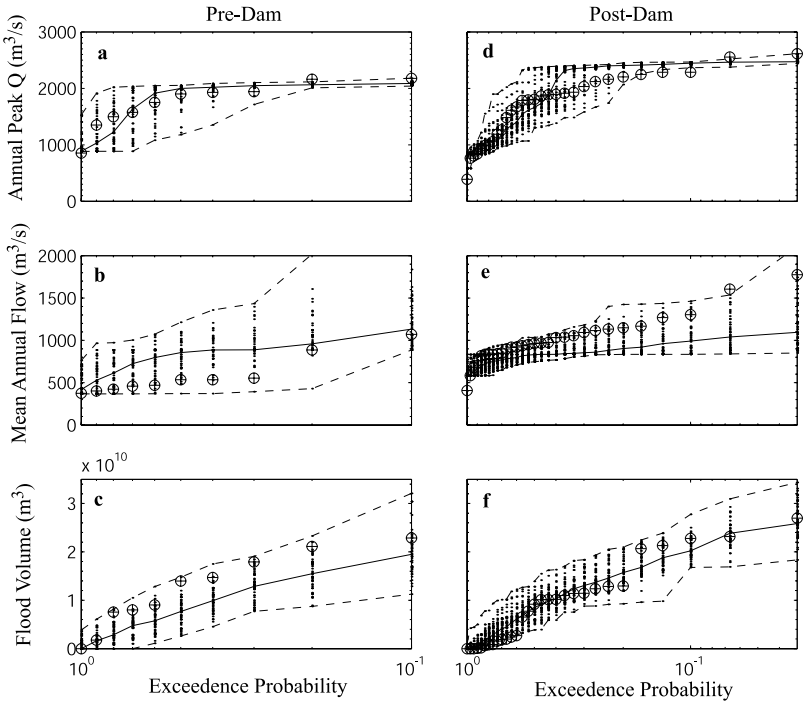

Figure 6. Predam cumulative probability plots of (a) annual maximum flood peaks, (b) mean annual flow (above wet season baseline discharge), and (c) flood volume (above wet season baseline discharge). (d, e, and f) Same as Figures 6a–6c but for the postdam simulations. Data for the verification gauge at Verona are shown as crosshairs, and the simulated series from 50 predam HYDROCARLO simulations are shown as dots. Dashed lines represent the simulation ranges, and solid lines represent the median value of simulations, or central tendency.

why we chose to verify the program against observed data for the main stem.

3.4.1. Predam Simulations

[48] In predam simulations we verified HYDROCARLO at Verona using data from 1933 to1943 (the entire predam period of record at this gauge). Verona is the only main stem gauge near the basin outlet and upstream of the delta with historical streamflow records prior to dam construction. The predam simulations in the program were run using data from the following gauges: Antelope Creek, Bend Bridge, Butte Creek, Deer Creek, Elder Creek, Mill Creek, Feather River, Stony Creek, and Thomes Creek (Figure 5). The predam inflow data for tributaries upstream of Bend Bridge amounted to <10 years of daily data, so we replaced these upstream tributaries with the gauging records from Bend Bridge itself (52 years of predam data). We included tributary input from HYDROCARLO simulations of Cow and Cottonwood Creeks to account for ungauged drainage area.

3.4.2. Postdam Scenario

[49] For the postdam scenario we verified HYDROCARLO at Verona and Freeport (Figure 5) using data from the period following major dam construction in the basin (i.e., 1970–2000). The postdam simulations in HYDROCARLO were run using data from the following gauges: American River, Antelope Creek, Battle Creek, Butte Creek, Clear Creek, Cottonwood Creek, Cow Creek, Deer Creek, Elder Creek, Feather River, Keswick, Mill Creek, Stony Creek, and Thomes Creek (Figure 5). We included tributary input from American River (predam) in HYDROCARLO simulations to account for ungauged drainage area that is unaffected by impoundments. We have included no changes in the channel geometry between the predam and postdam eras because such data were not available.

3.5. Verification Results

[50] Numerous flow properties can be decomposed from any hydrograph, whether it is recorded or simulated. We have chosen six properties to verify HYDROCARLO's ability to simulate hydrographs that represent historical flood peak, duration, shape, and timing. However, this is by no means an exhaustive list of flow properties that can be extracted from HYDROCARLO's hydrographs. Although we have taken efforts to verify that HYDROCARLO predicts historical flow characteristics well on the main stem, the program is (like the flood frequency curve itself) essentially unverifiable. However, it is possible to validate the utility of the program in repeated applications to decision making in which it is found to be useful. In general, our simulations accurately describe the flow conditions recorded during the predam and postdam eras. From them we calculated a range and central tendency of all simulations for each era (Figures 6, 7, 8, and 9).

3.5.1. Annual Peak, Mean Annual Flow, and Flood Volume

[51] Figures 6 and 7 show the results of annual peak, mean annual flow, and flood volume for predam and postdam hydrographs generated by HYDROCARLO at Verona and Freeport, respectively. The historical flood peaks at Verona (Figure 6a) bound the simulated range of annual maximum peaks at the lowest and highest exceedence probabilities. The lower bound of simulated peaks at

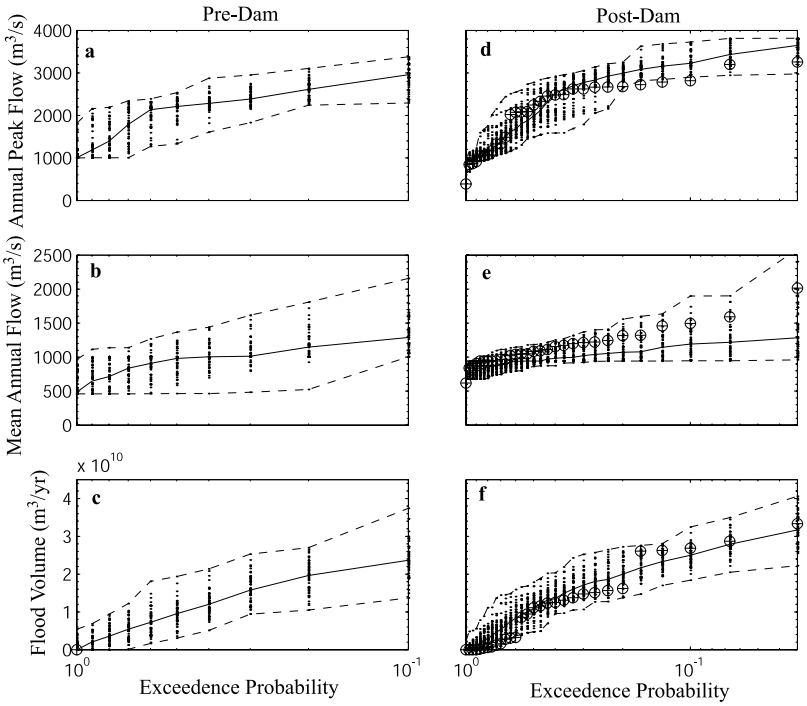

Figure 7. Predam cumulative probability plots of (a) annual maximum flood peaks, (b) mean annual flow above wet season baseline discharge, and (c) flood volume (above wet season baseline discharge). (d, e, and f) Same as Figures 7a–7c but for the postdam simulations. Data for the verification gauge at Freeport (postdam only) are shown as crosshairs, and the simulated series from 50 predam HYDROCARLO simulations are shown as dots. Dashed lines represent the simulation ranges, and solid lines represent the median value of simulations, or central tendency.

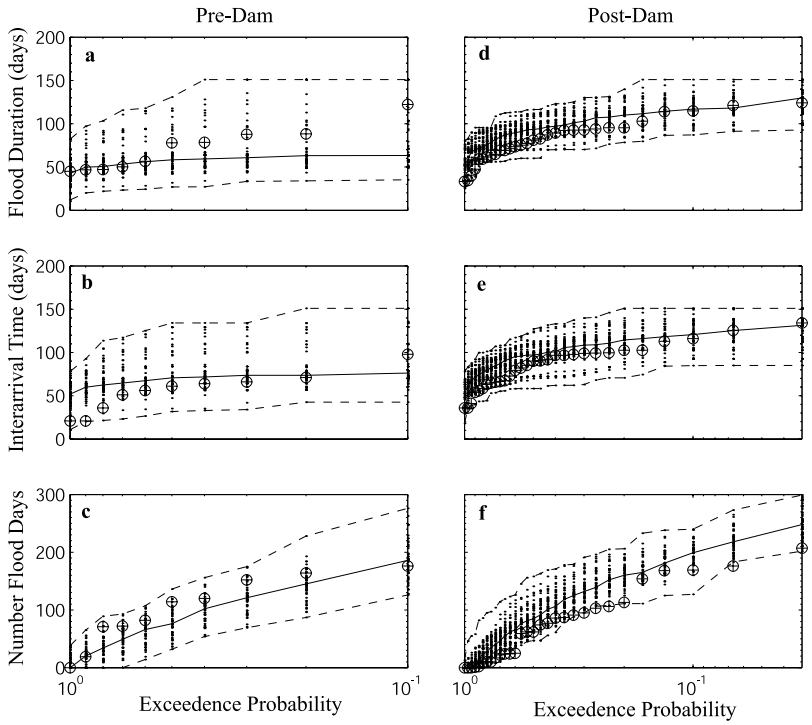

Figure 8. Predam cumulative probability plots of (a) mean flood duration, (b) mean interarrival time, and (c) number of flood days. (d, e, and f) Same as Figures 8a–8c but for postdam simulations. Data for the validation gauge at Verona are shown as crosshairs, and the simulated series from 50 predam HYDROCARLO simulations are shown as dots. Dashed lines represent the simulation ranges, and solid lines represent the median value of simulations, or central tendency.

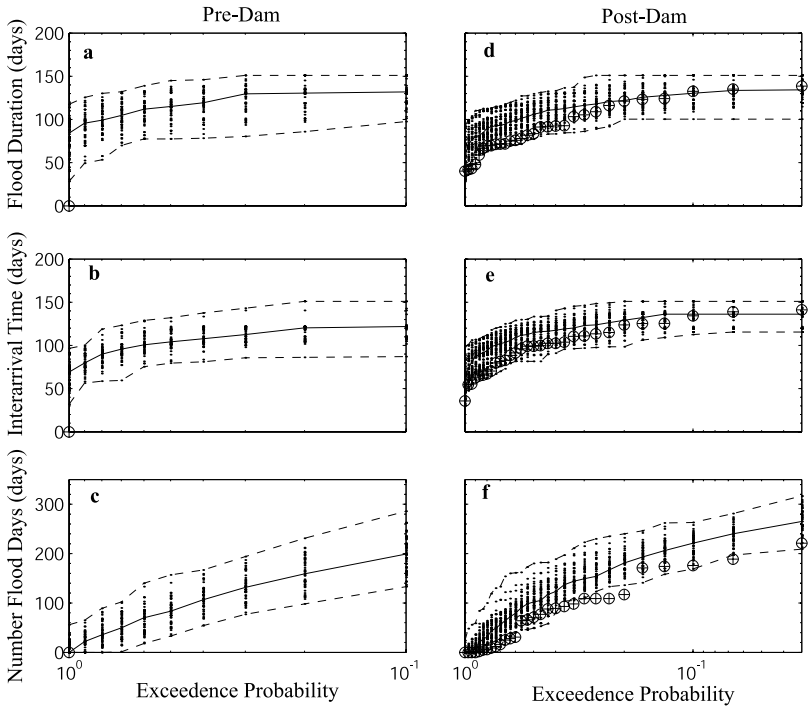

Figure 9. Predam cumulative probability plots of (a) mean flood duration, (b) mean interarrival time, and (c) number of flood days. (d, e, and f) Same as Figures 9a–9c but for postdam simulations. Data for the validation gauge at Freeport (postdam only) are shown as crosshairs, and the simulated series from 50 predam HYDROCARLO simulations are shown as dots. Dashed lines represent the simulation ranges, and solid lines represent the median value of simulations, or central tendency.

the highest exceedence probability, or the flow most frequently exceeded, is set to the value of combined routed wet season baseline discharge from all tributaries, which is slightly higher than the lowest historical annual peak. However, this is not a concern because HYDROCARLO was developed to simulate flows above baseline discharge. At the lowest exceedence probability the simulated flood peak at Verona is asymptotic to 2178 $m^3 s^{-1}$ in the predam era (Figure 6a) and 2614 $m^3 s^{-1}$ in the postdam era (Figure 6d). These values represent the thresholds of flood flow, above which flow spills over Fremont Weir. The weir constrains the variability of annual maximum flows upward of 2000 $m^3 s^{-1}$ to a narrow range. This is the reason that the simulated range (i.e., the uncertainty) does not increase at the lowest exceedence probabilities, as would be expected in the flood frequency curve for a river reach devoid of flood control weirs. It is noteworthy that predam peaks of flow within the leveed channel at Verona are lower than postdam ones, and this matter is discussed below. Otherwise, predam and postdam simulated flood peaks bound the historical data and illustrate the potential range of variability, especially for flows of intermediate frequencies that transport most sediment [*Singer and Dunne*, 2001] and drive important ecological processes [*Mahoney and Rood*, 1998; *Milhous*, 1998; *Pitlick and Van Steeter*, 1998; *Johnson*, 2000]. HYDROCARLO simulations generally bracket historical flood peaks at Verona for other exceedence probabilities.

[52] There are no predam historical data available for Freeport, but we simulated predam flows at this location (Figures 7a–7c). The postdam simulations generally bracket the annual historical postdam peaks. There is a larger simulated range in flood peaks for the lowest exceedence probabilities at Freeport compared with Verona (compare Figures 6d and 7d) because of the variable influence of the American River (Figure 5) and the smaller effect its upstream weir has on flow in the main channel (Sacramento Weir has less than one third the spill capacity of Fremont Weir).

[53] Simulated medians for many hydrograph characteristics appear to fall consistently below or above historical data for a range of exceedence probabilities (e.g., predam median annual peaks at Verona are consistently higher than historical data for probabilities ranging from 0.4 to 0.2). At this point, we cannot explain the systematic biases in the simulations with respect to the historical data. We have not yet conducted a sensitivity analysis of model parameters but discuss model conditioning and parameter sensitivity below (in section 3.6.4). It should be noted that we conducted no model calibration to arrive at the results presented herein.

[54] Simulations of mean annual flow and flood volume at Verona and Freeport generally bound historical data (Figures 6b, 6e, and 7e). It appears that mean annual flow at Verona has increased slightly in the postdam era concomitant with the increase in annual peaks, and our simulations reflect that change. Flood volumes appear to have changed very little between the predam and postdam eras (Figures 6c and 6f), except that the longer record in the postdam era has sampled larger flood volumes at the lowest exceedence probabilities, thereby better reflecting the flow variability.

3.5.2. Flood Duration, Interarrival Time, and Number of Flood Days

[55] Figures 8 and 9 show the results of three more probability checks on predam and postdam hydrographs generated by HYDROCARLO at Verona and Freeport,

respectively. Again, HYDROCARLO simulations generally bracket the historical data in each plot. Flood duration at Verona appears to have decreased slightly between the predam and postdam eras for the 0.1 exceedence probability. However, the historical value of flood duration at this probability in the predam era is essentially the same as that of 0.03 for the postdam era. The shift in the exceedence probability in flood duration between eras is probably due to the difference between the effect of flood attenuation by upstream floodplains in the predam era and upstream flood control dams in the postdam era. Specifically, dams appear to have decreased flood duration for large floods, although the short predam historical record limits a more direct comparison. A similar story emerges for number of flood days at Verona (Figures 8c and 8f). Because we are making computations on a daily time step, it follows that a reduction in flood duration leads to a reduction in the number of flood days. Interarrival times have increased between eras (compare Figures 8b and 8e), perhaps because of the effects of flood control in damping out the smallest flood peaks. This effect is replicated between our predam and postdam simulations at Freeport (Figures 9b and 9e).

3.6. Applications

3.6.1. Simulating Flow at Ungauged Main Stem Locations

[56] Estimates of flow properties at ungauged main stem locations are required for a number of purposes. In engineering applications, point estimates of peak flow and total annual flow volume may be needed to design flood control levees and diversion structures. Estimates of sediment transport and hydrograph fluctuation may be important in determining the operational capacity and longevity of such engineering works. In geomorphic applications, local flow estimates are required to assess thresholds for sediment transport, to route sediment through river reaches, and to model sediment concentration, floodplain inundation, and floodplain sedimentation. In ecological applications, local estimates of instream flow and overbank flow may be required to assess quality of fish and benthic habitat and inundation regimes of riparian habitats, respectively. Estimates of sediment transport may also be required to calculate the frequency of flushing flows and general habitat disturbance. Rates of drawdown may be needed to test whether riparian seedlings in a particular area could viably germinate and establish themselves on floodplains.

[57] In the absence of detailed hydrographs at particular locations, estimates of flow properties are generally transferred from the closest streamflow gauge, which might be tens of river kilometers away and possess very different hydraulic conditions from the site in question. HYDROCARLO can provide flow estimates at the relevant locations for a variety of at-a-point analyses.

3.6.2. Assessing Risk in a Fluvial System

[58] The concept of risk has been used to describe hazard, expected loss, or the probability of an outcome [*U.S. Army Corps of Engineers*, 1992]. Risk analysis is currently used in design and maintenance of flood control levees [*National Research Council*, 2000] and in design of dam and storage facilities [*Federal Energy Regulatory Commission*, 1993]. Analysis of potential outcomes has utility in applications of sediment transport and the restoration of aquatic and riparian habitats, which are generally sensitive to various hydrograph components, including magnitude, frequency, timing, duration, and rate of change [*Poff et al.*, 1997].

[59] For example, in order for riparian cottonwood seedlings to successfully germinate and recruit they require a flood pulse sufficient to wet the floodplain surface for seed deposition [*Mahoney and Rood*, 1998]. Once this flood peak occurs, seedling survival depends on drawdown rate, such that saturated sites are exposed for seedling establishment and growing roots maintain contact with the capillary fringe on the water table. Although cottonwood roots grow anywhere from 0.5 to 1.0 cm d^{-1}, a maximum survivable rate of water table decline is $\sim$2.5 cm d^{-1} [*Mahoney and Rood*, 1998]. Existing methods for analyzing flow at ungauged locations are limited and often involve the use of pressure transducers to infer stage over a single flood season (J. Stella, University of California, Berkeley, personal communication, 2001). Such a strategy provides little guidance in evaluating the likelihood of favorable rates of recession in the season of riparian seedling germination because the historical record is relatively short.

[60] HYDROCARLO may be used to assess whether hydrologic conditions for a particular place are suitable for the establishment and recruitment of cottonwoods. It may also be used to evaluate the probability of successful cottonwood recruitment. For example, we simulated annual peak stages and recessions for a potential ungauged cottonwood recruitment site north of Tehama $\sim$3 km downstream of Elder Creek confluence (Figure 5) between April and May (the period April though mid-June was identified as the cottonwood germination season in the nearby San Joaquin River basin (J. Stella, University of California, Berkeley, personal communication, 2001)) using predam and postdam flow regimes. Figure 10a shows that under the predam flow regime, the stage necessary for flow to access the floodplain (68.7 m) was exceeded $\sim$30% of the time, indicated by the median, whereas it was rarely if ever exceeded in the postdam flow regime (Figure 10c). The implication is that the current flow regime is not viable for the establishment of cottonwood seedlings. Figure 10b shows that in the predam flow regime the maximum drawdown rate of 2.5 cm d^{-1} is exceeded $\sim$10% of the time. In the postdam flow regime, however, the maximum drawdown rate is exceeded approximately 45% of the time (Figure 10d) during the critical period of seedling root growth [*Mahoney and Rood*, 1998]. Thus the current flow regime is not conducive to the establishment of cottonwoods and may be a severe limit on their subsequent growth. Although this is a preliminary result requiring more rigorous analysis of local cottonwoods, it is clear that some type of flow alteration would be necessary to restore cottonwood stands in this floodplain location.

3.6.3. Using HYDROCARLO to Detect Bed Level Change

[61] The use of HYDROCARLO simulations within HEC-RAS has led to new insights into the relationship between flood control structures and bed level in the Lower Sacramento River. The following discussion illustrates how the application of a stochastic program to a fluvial system highlighted a long-term change in the fluvial system.

3.6.3.1. Evidence

[62] The Sacramento flood control system was designed to shunt flow above certain thresholds through weirs into

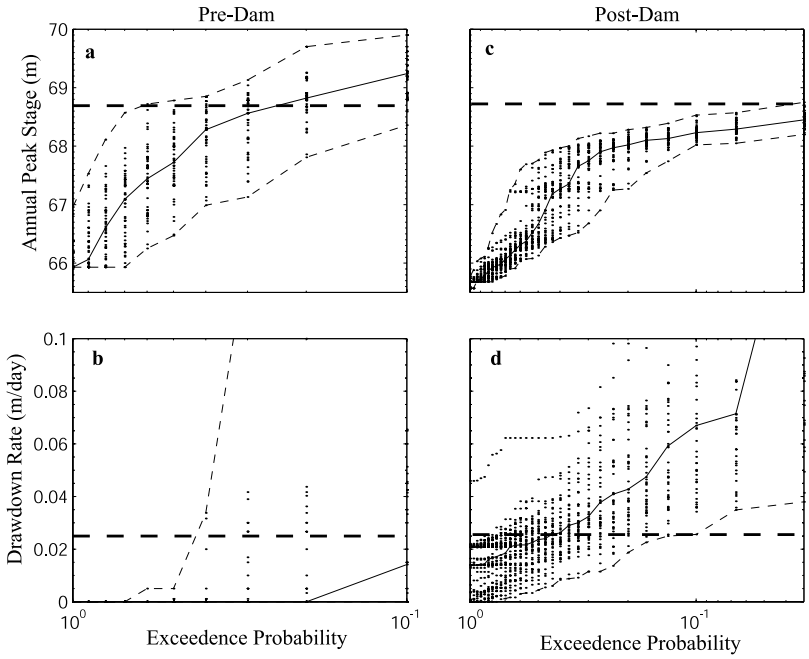

Figure 10. Annual peak stage at Tehama (below the Elder Creek confluence) in the (a) predam era and (c) postdam era. Dashed line represents the stage necessary to access the floodplain. Mean rate of drawdown at the same site is shown for the (b) predam and (d) postdam eras. The dashed lines here represent the maximum survivable rate of 2.5 cm d^{-1} of cottonwood seedlings [*Mahoney and Rood*, 1998]. The plots illustrate the effect of dam operations on flow conditions necessary for cottonwood establishment and recruitment. Note that the upper dashed bound is not shown on Figure 10d because it is beyond the displayed scale.

bypasses that eventually drain to the San Francisco-Sacramento-San Joaquin Bay Delta. Thus as flow from upstream increases above the threshold for flow over a particular weir, there should be ever larger increases in flow over the weir compared with flow increases through the main stem downstream of the weir. Since flow in the main stem is published as mean daily discharge, smaller and smaller increments of flow increase at a main stem gauge downstream would tend to be asymptotic to a particular value of discharge. The flood frequency (of annual maximum peak flows) at a gauging station downstream of the flood weir can thus be thought of as asymptotic to the discharge at which increasing flow from upstream would cause no increase at that gauge. This asymptote should be more or less steady through time as long as there are no modifications to the flood control system, significant changes in roughness, or bed level changes. If the channel bed were to erode significantly, the connection between main stem channel flow and flow passing over the weir would be altered. Larger discharges would reach the downstream gauge, causing the asymptote to shift upward. Figure 11 illustrates how bed level changes could alter flood levels and change the functioning of the flood control system. With increased channel bed erosion the flow depth at which the weir is overtopped increases, and higher peak flows pass downstream through the main channel.

[63] Inspection of predam and postdam historical flood peaks at Verona shows larger flows in the postdam era than in the predam one (crosshairs in Figures 6a and 6d). However, this seems counterintuitive given that dams have been operated to control the largest flood peaks. Working under this assumption alone, one could only surmise that the predam historical period represented in this analysis was one of anomalously low flood peaks compared to the postdam one. Our predam simulations from HYDROCARLO, however, utilized high flood flows from each tributary and especially at the upstream boundary condition of Bend Bridge. However, these higher discharge boundary conditions did not elevate main stem flood peaks at Verona beyond those of the historical data for the lowest exceedence probabilities because they were shunted out of the model space in HEC-RAS simulations via Fremont Weir upstream of the gauge. Other possibilities for the higher flood peak asymptote in the postdam era include alterations to the flood control system, significant change in roughness, and bed level change. There have been no major alterations to the flood control system [*U.S. Army Corps of Engineers*, 1998], and we know of no conditions that would have altered roughness. A previous study documented a decrease in specific gauge records in the Sacramento River between Knights Landing and Sacramento over ~20 years [*Water Engineering and Technology*, 1990], and we calculated an average erosion rate for this reach of 1.7 cm yr^{-1} for the time period 1948–1979 from the sediment transport budget [*Singer and Dunne*, 2001].

3.6.3.2. Procedure

[64] We simulated 50 ten-year program runs (predam) and 50 thirty-year program runs (postdam) to identify the asymptote at Verona for each era. Then we selected one simulation in each era that is asymptotic to the highest simulated peak flow and saved its boundary conditions (i.e., inflow hydrographs) in HEC-RAS. Next, we ran more

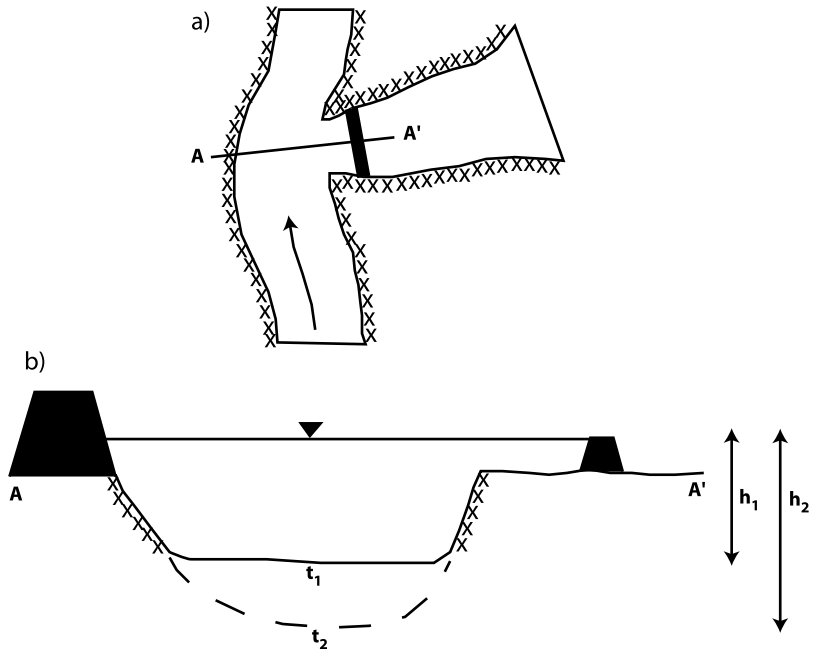

Figure 11. Schematic showing (a) planform view of leveed main channel reach with a flood weir leading to a bypass and (b) cross-sectional view of how flood control system could become impaired by incision of the channel bed. Bed levels before (t_1) and after (t_2) erosion are shown along with water levels necessary to overtop the weir before (h_1) and after (h_2) incision.

HEC-RAS simulations with these same inflow hydrographs while adjusting the elevation of Fremont Weir (rather than adjusting the bed elevation at each cross section) until the simulated asymptote equaled that of the historical data (i.e., predam peak = 2178 m^3 s^{-1} and postdam peak = 2614 m^3 s^{-1}). In other words, we zeroed HEC-RAS so that historical data and simulations for a particular era had a common flood asymptote (or in this case, a common elevation for Fremont Weir). Once the asymptotes matched for a particular era, we reran all the simulations and used the resulting simulations for program verification (section 3.5).

3.6.3.3. Erosion Rate

[65] Since simulations for each era were zeroed (i.e., the elevation of Fremont Weir was fixed to equalize historical and simulated high flow asymptotes), we could calculate the difference in the elevation of Fremont Weir between eras. We divided this elevation difference by the number of years between the eras to arrive at an average annual erosion rate for this reach of river in intervening period. This result is 2.1 cm yr^{-1} (79 cm between the first year of each era, 1933 and 1970), which is close to the 1.7 cm yr^{-1} rate for the period 1948–1979, independently predicted in our analysis of suspended sediment transport [*Singer and Dunne*, 2001]. This erosion trend is corroborated by flow data from the Fremont Weir Spill. Figure 12 shows that from 1955 to 1975, there was a progressive change in the partitioning of water between the main channel and the flow over the weir. For example, the weir spill diminished from ~4300 m^3 s^{-1} between 1955 and 1957 to ~1000 m^3 s^{-1} between 1973 and 1975 for a main stem flow of ~1850 m^3 s^{-1} at Verona. Likewise, main stem flow at Verona increased from ~1600 m^3 s^{-1} between 1949 and 1951 to ~1850 m^3 s^{-1} between 1973 and 1975 for Fremont Weir spill of ~1000 m^3 s^{-1}. Although there are clearly episodes of erosion and deposition in this reach, there is an apparent trend of erosion that persisted over 25 years. Over this same period, there is a weakly increasing trend in combined annual peak discharge from Fremont Weir spill and Verona (R^2 = 0.31 and p = 0.22), indicating that changes in the partitioning of water between the weir and the main stem are not due to diminished flood flow.

[66] Figure 13 shows a frequency plot of predam and postdam historical flood peaks (open circles) and one simulation with an asymptote zeroed to that of the historical value (pluses). We then altered the elevation of Fremont Weir for flood-routing simulations, assuming the constant bed erosion rate. Figure 13 (top) shows how boundary conditions from a predam simulation (beginning in 1933) would look after being routed through the river channel of the postdam era (beginning in 1970). Remarkably, routing high predam flows through the postdam channel (i.e., with lowered bed level equal to that of the postdam era) produces peak discharges asymptotic to the same peak flow that was recorded in the postdam era (~2500 m^3 s^{-1}). If the erosion trend were to continue into the future, the same flood frequency regime in the tributaries and upper main stem would pass progressively larger floods to the lower Sacramento.

3.6.3.4. Implications

[67] These results have implications for flood control in the lower Sacramento. First, flood control dams have had very little impact on the largest peak flows in the leveed channel of the lower Sacramento River. We have demonstrated by normalizing flow for changes in bed elevation that peak flows in the postdam era are approximately the same as those in the predam era. In other words, flood control dams in the Sacramento basin do not diminish the largest peak floods traveling through the channel of the lower river. The *U.S. Army Corps of Engineers* [1998] documented that flows discharged from Shasta Dam take

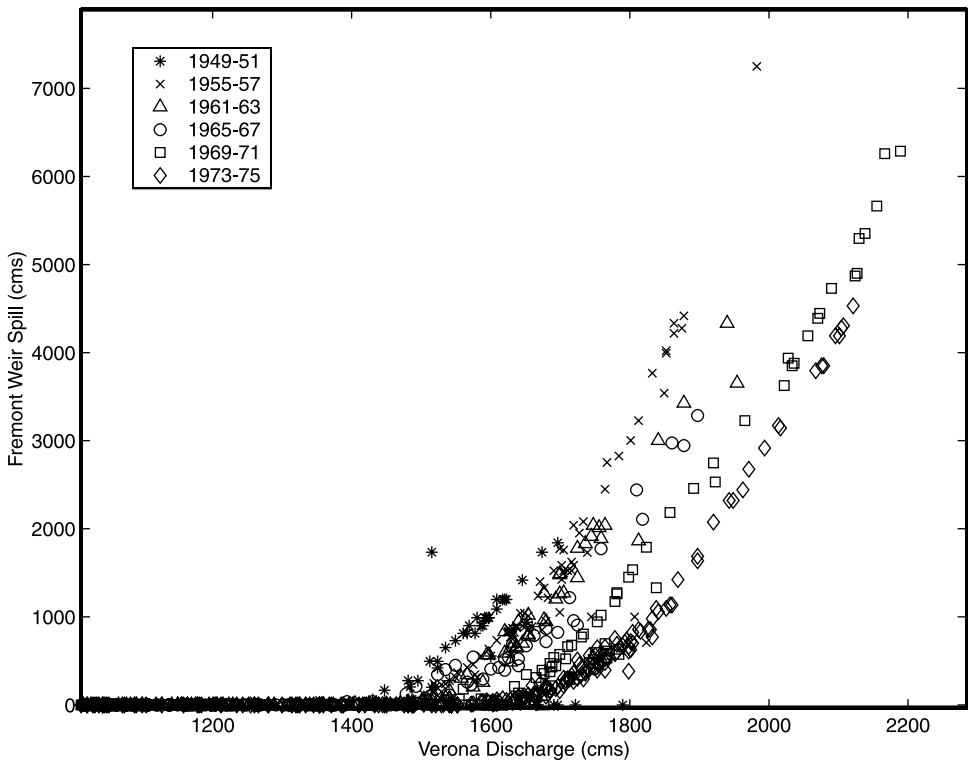

Figure 12. Plot showing declining flow over Fremont Weir compared with flow at Verona on the main stem downstream of the weir from 1949 to 1975.

62 hours to reach Verona. As a result, high flows may be released from Shasta prior to the arrival of a large, swift rainstorm in the lower Sacramento Valley. Such a rainstorm may cause increased flood discharges from the lower Feather River basin, for example, to arrive at its confluence with the Sacramento concurrent with the high-flow release from Shasta. This inefficiency in flood control would be inherent in any basin where flood control dams are located at the outer edges of a large valley and where large and swift storms are generated in the lower part of the basin.

[68] Second, although channel capacity increases with incision, there is nevertheless an increase in flood risk for areas outside the levees of the lower Sacramento. Incision can expose unprotected and permeable banks (i.e., below riprap and levees) and weaken aged levee materials. Flow from the main channel can seep under or through porous levee materials and emerge from the floodplain outside the levee. Perched water tables and evidence of boils and piping have been reported outside the East Levee along Pocket Road in the city of Sacramento in the reach between Verona and Freeport (M. Salvador, CDWR, personal communication, 2001). Incision can also focus shear stress at the toe of riprap or a levee and weaken the engineering structure by undercutting its toe. Such a scenario could eventually lead to levee break and catastrophic flooding in a populated area.

3.6.4. Adapting HYDROCARLO

[69] HYDROCARLO is an empirical-stochastic program applicable to large river basins for which streamflow data are spatially and temporally abundant. The program's predictive capability is increased by the length of synchronous records for each major tributary in a basin and by records that represent a large range of flood events that could occur at a particular station. HYDROCARLO was verified in a

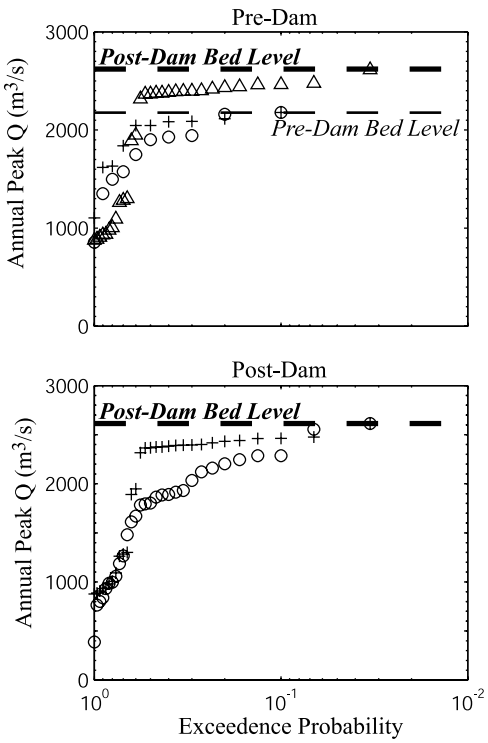

Figure 13. Plot showing simulations with the flow asymptote (pluses) zeroed to that of the historical data (open circles) for a particular era by adjusting the elevation of Fremont Weir. The plot shows (top) predam and (bottom) postdam hydrology at Verona. Triangles (Figure 13, top) show how simulated predam data would look at the postdam bed level beside which Fremont Weir would be 0.79 m higher.

simple way herein by comparing simulated output with observed data for various hydrograph characteristics. We assigned HYDROCARLO's three parameters (i.e., baseline discharge, ABC, and number of bins) according to simple, repeatable rules, which we developed to represent flood thresholds and the complexity of cross correlations in flow series between gauges in the Sacramento basin (we expect that these rules would be altered before the program is applied to a different basin). Although we conducted no parameter fitting or other calibration, we were able to reasonably reproduce observed main stem hydrographs. This suggests that either the program is not very sensitive to these parameters or we created excellent rules. The former is more likely because of the program's reliance on observed data sampled in a Monte Carlo fashion, but HYDROCARLO's sensitivity to the rules may also be investigated. Although such an analysis is beyond the scope of this paper, it would be useful to determine which rules should be most carefully specified. The program could be thus conditioned to perform well for a given basin and to ensure the program is robust and widely applicable. We suggest a simple stepwise three-stage process of parameter specification that at each stage would be assessed by a set of diagnostics comparing simulated/routed and observed flow, such as that presented in section 3.5.

[70] The first rule computes the flood threshold via LOWESS [*Cleveland*, 1979] at each gauge. Various other statistical determinations of the flood threshold could be specified. For example, one might divide flow series into flood and nonflood days via its mean or by more sophisticated flow separation methods. These variations in the flood threshold at each tributary gauge could then be assessed in terms of their combined effect on flow characteristics at the basin outlet.

[71] The second rule computes across-basin correlation between synchronous flood peaks at the two most distant gauges. ABC could be specified according to more complex basin-wide rules. If, for instance, the user determined that ABC were particularly high between the most distant gauges but assumed there was some reason other than basin-wide storms for correlation between these gauges, then this information could be used to assess across-basin correlation. For example, in a large river basin that spans a wide range of latitude, flood event ranks at the two most distant gauges might lie along an east-west axis and therefore be correlated according to latitude. In this case, across-basin correlation could be tested between flood peaks from gauging stations farthest from each other in the north-south direction instead of those farthest in absolute distance. One could compute ABC according to various hypotheses of the influence of basin-wide storms and assess their effect on flow at the basin outlet.

[72] The third rule uses the ABC to divide the flood matrices into a number of bins for flood selection. The number of bins used in HYDROCARLO was set herein using ABC, a measure assumed to represent the relationship between all gauges in the basin. This assumption may be relaxed to account for local relationships between gauges by varying the number of bins used. For example, if across-basin correlation were low (<0.25) between the most distant gauges but it was assumed that correlation was higher between some gauges in the network, one bin for flood event selection over the entire basin would be insufficient to represent this relationship. To rectify this problem, the user could test for correlation between each gauge and every other gauge in the basin to develop a system of look-up tables containing differing numbers of bins. For example, if the correlations in synchronous flood peaks (1) between gauge 3 and gauges 4, 5, and 6 were 0.4, 0.6, and 0.8, respectively, flood events would be chosen at gauges 4, 5, and 6 from two, three, and four bins, respectively (Figure 1). The number of bins for each correlation range (and the correlation ranges themselves) could also be altered to reflect more complexity in a particular river basin. Each new specification of the rule for number of bins should be tested against a separate set of flow data near the basin outlet.

[73] Specification of the aforementioned parameters should proceed in an iterative, stepwise fashion, in which a single parameter is specified according to a rule. The program's response to each change in the rule would be measured. Once a set of hypothesized rules is exhausted, the one that produced the best results would be selected, and this procedure would repeat for the remaining parameters. As such, HYDROCARLO could be simultaneously conditioned for a use in a given basin and tested for sensitivity to specified rules.

[74] Finally, HYDROCARLO's predictive capability could be improved by augmenting historical streamflow records with synthetic hydrographs for extreme floods using data from ancillary sources. This has been recommended to better capture hydrologic trends and the statistical distribution of natural phenomena [*National Research Council*, 1991; *Archer*, 1999]. Flood event selection at any tributary is limited at the upper end of the distribution (i.e., at the lowest exceedence probability) by the largest flood event of record. Field evidence has demonstrated, however, that events larger than those recorded have likely occurred in the past, and such events are likely to occur again in the future [*Baker et al.*, 2002]. Therefore estimated hydrographs constructed for such floods should be added to the historical record from which HYDROCARLO selects events in order to widen the range of possible flood events and represent potential events that have not been recorded. Estimates of peak flow can be made by a variety of paleohydrological proxies including tree ring analysis, palynology, fluvial deposits, and surveys of tributary channel dimensions. These techniques provide guidance in estimating hydrographs that represent extreme flood conditions in a particular river system. However, the technique for adding these large floods to the flood matrix (Figure 3) with the appropriate frequency requires further research.

4. Conclusion

[75] The HYDROCARLO stochastic streamflow generator stochastically represents spatiotemporal patterns in tributary inflow by incorporating the seasonality in flow and the correlation in flood event occurrence and flood peak magnitude that are reflected in historical streamflow records. It produces simulated sets of synchronous tributary inflow to a large river. We applied the program to the Sacramento River Basin, utilizing tributary flows to simulate main stem hydrology. We conducted preliminary verification of the program by comparing the frequency of various

hydrograph characteristics from the simulated series with those from historical records at main stem gauging points for predam and postdam flow scenarios. The program produces output that can be used for numerous applications including simulating flows at ungauged main stem locations, assessing flood risk, characterizing the flooding regimes in ways that are relevant for ecosystem functioning, and detecting bed level change. HYDROCARLO may be adapted for different hydroclimates, and its predictive capability could be improved by incorporating synthetic hydrographs of unrecorded extreme floods at tributary gauges.

[76] **Acknowledgments.** We thank Emmanuel Gabet and James Kirchner for assisting in the early stages of the program's development, Jonathan Stock for comments on an early version of the manuscript, and John Stella for discussions on ecological applications. Data were provided by Ken Dickerson, Russell Eckman, Tanya Ehorn, and Dwight Russell of California Department of Water Resources, Jason Schwenkler of Chico State University, and Jeff Harris (formerly) of the U.S. Army Corps of Engineers. A consulting report by the firm of Jones and Stokes first suggested erosion in the lower Sacramento. We acknowledge the comments of four anonymous reviewers and the support of CALFED grant 4600002659 and NASA grant NAG5-8396.

References

Archer, D. (1999), Practical application of historical flood information to flood estimation, in *Hydrological Extremes: Understanding, Predicting, Mitigating*, edited by L. Gottschalk et al., *IAHS Publ.*, *255*, 191–199.

Baker, V. R., R. H. Webb, and P. K. House (2002), The scientific and societal value of paleoflood hydrology, in *Ancient Floods, Modern Hazards: Principles and Applications of Paleoflood Hydrology*, *Water Sci. Appl. Ser.*, vol. 5, edited by P. K. House et al., pp. 1–19, AGU, Washington, D. C.

Barkau, R. (1997), One-dimensional unsteady flow through a full network of open channels, manual, U.S. Army Corps of Eng., Davis, Calif.

Benson, M. A., and N. C. Matalas (1967), Synthetic hydrology based on regional statistical parameters, *Water Resour. Res.*, *3*(4), 931–935.

Beven, K. J. (2000), *Rainfall-Runoff Modelling, A Primer*, 360 pp., John Wiley, Hoboken, N. J.

Brunner, G. W., and V. Bonner (1994), HEC river analysis system (HEC-RAS), technical report, Hydrol. Eng. Cent., Davis, Calif.

Burnash, R. J. C., R. L. Ferral, and R. A. McGuire (1973), A generalized streamflow simulation system: Conceptual modeling for digital computers, technical report, 204 pp., Natl. Weather Serv., Sacramento, Calif.

Church, M., and M. A. Hassan (1992), Size and distance of travel of unconstrained clasts on a streambed, *Water Resour. Res.*, *28*(1), 299–303.

Cleveland, W. S. (1979), Robust locally weighted regression and smoothing scatterplots, *J. Am. Stat. Assoc.*, *74*, 829–836.

Earle, C. J., and H. C. Gritts (1986), Reconstructing riverflow in the Sacramento basin since 1560, technical report, Lab. of Tree-Ring Res., Tucson, Ariz.

Federal Energy Regulatory Commission (1993), Engineering Guidelines for the evaluation of hydropower projects, Washington, D. C.

Fiering, M. B. (1967), *Streamflow Synthesis*, 139 pp., Harvard Univ. Press, Cambridge, Mass.

Gilbert, G. K. (1917), Hydraulic-mining debris in the Sierra Nevada, report, U.S. Geol. Surv., Menlo Park, Calif.

Gleick, P. H. (1987), The development and testing of a water balance model for climate impact assessment: Modeling the Sacramento basin, *Water Resour. Res.*, *23*(6), 1049–1061.

Hannan, E. J. (1955), A test for singularities in Sydney rainfall, *Aust. J. Phys.*, *8*(2), 289–297.

Hirschboeck, K. K. (1987), Hydroclimatically-defined mixed distributions in partial duration flood series, in *International Symposium on Flood Frequency and Risk Analyses*, edited by V. P. Singh, pp. 199–212, D. Reidel, Norwell, Mass.

Hirschboeck, K. K. (1988), Flood hydroclimatology, in *Flood Geomorphology*, edited by V. R. Baker, R. C. Kochel, and P. C. Patton, pp. 27–49, John Wiley, Hoboken, N. J.

Ingram, B. L., J. C. Ingle, and M. E. Conrad (1996), A 2000 yr record of Sacramento-San Joaquin river inflow to San Francisco Bay estuary, California, *Geology*, *24*(4), 331–334.

Johnson, W. C. (2000), Tree recruitment and survival in rivers: Influence of hydrological processes, *Hydrol. Processes*, *14*, 3051–3074.

Jones, B. L., N. L. Hawley, and J. R. Crippen (1972), Sediment transport in the western tributaries of the Sacramento River, California, report, U.S. Geol. Surv., Washington, D. C.

Junk, W. J., P. B. Bayley, and R. E. Sparks (1989), The flood pulse concept, in *Proceedings of International Large River Symposium*, *Can. Fish. Aquat. Sci. Spec. Publ.*, vol. 106, edited by D. P. Dodge, pp. 110–127, Dep. of Fish. and Oceans, Ottawa, Ontario, Canada.

Kelley, R. (1998), *Battling the Inland Sea*, 395 pp., Univ. of Calif. Press, Berkeley.

Lettenmaier, D. P., and T. Y. Gan (1990), Hydrologic sensitivities of the Sacramento-San Joaquin River basin, California, to global warming, *Water Resour. Res.*, *26*(1), 69–86.

Lettenmaier, D. P., and D. P. Sheer (1991), Climatic sensitivity of California water resources, *J. Water Resour. Plann. Manage.*, *117*(1), 108–125.

Mahoney, J. M., and S. B. Rood (1998), Streamflow requirements for cottonwood seedling recruitment—An integrative model, *Wetlands*, *18*(4), 634–645.

McLean, D. G., M. Church, and B. Tassone (1999), Sediment transport along lower Fraser River: 1. Measurements and hydraulic computations, *Water Resour. Res.*, *35*(8), 2533–2548.

Milhous, R. T. (1998), Modelling of instream flow needs: The link between sediment and aquatic habitat, *Regul. Rivers Res. Manage.*, *14*, 79–94.

National Research Council (1988), *Estimating Probabilities of Extreme Floods: Methods and Recommended Research*, 141 pp., Natl. Acad. Press, Washington, D.C.

National Research Council (1991), *Opportunities in the Hydrologic Sciences*, 348 pp., Natl. Acad. Press, Washington, D. C.

National Research Council (2000), *Risk Analysis and Uncertainty in Flood Damage Reduction Studies*, 202 pp., Natl. Acad. Press, Washington, D. C.

National Research Council (2001), *Future Roles and Opportunities for the U.S. Geological Survey*, 179 pp., Natl. Acad. Press, Washington, D. C.

Nijssen, B., and D. P. Lettenmaier (1997), Streamflow simulation for continental-scale river basins, *Water Resour. Res.*, *33*(4), 711–724.

Pitlick, J., and M. M. Van Steeter (1998), Geomorphology and endangered fish habitats in the upper Colorado River: 2. Linking sediment transport to habitat maintenance, *Water Resour. Res.*, *34*(2), 303–316.

Poff, N. L., J. D. Allan, M. B. Bain, J. R. Karr, K. L. Prestegaard, B. D. Richter, R. E. Sparks, and J. C. Stromberg (1997), The natural flow regime, *Bioscience*, *47*(11), 769–784.

Richards, K., J. Brasington, and F. Hughes (2002), Geomorphic dynamics of floodplains: Ecological implications and a potential modelling strategy, *Freshwater Biol.*, *47*, 559–579.

Richter, B. D., J. V. Baumgartner, J. Powell, and D. P. Braun (1996), A method for assessing hydrologic alteration within ecosystems, *Conserv. Biol.*, *10*(4), 1163–1174.

Risbey, J. S., and D. Entekhabi (1996), Observed Sacramento Basin streamflow response to precipitation and temperature changes and its relevance to climate impact studies, *J. Hydrol.*, *184*, 209–223.

Rodriguez-Iturbe, I., D. R. Cox, and V. Isham (1987), Some models for rainfall based on stochastic point processes, *Proc. R. Soc. London, Ser. A*, *410*, 269–288.

Singer, M. B., and T. Dunne (2001), Identifying eroding and depositional reaches of valley by analysis of suspended-sediment transport in the Sacramento River, California, *Water Resour. Res.*, *37*(12), 3371–3381.

Stedinger, J. R., and M. R. Taylor (1982), Synthetic streamflow generation: 1. Model verification and validation, *Water Resour. Res.*, *18*(4), 909–918.

Sudler, C. E. (1927), Storage required for the regulation of streamflow, *Trans. Am. Soc. Civ. Eng.*, *91*, 622–660.

Thompson, K. (1960), Historical flooding in the Sacramento Valley, *Pac. Hist. Rev.*, *29*, 349–360.

Tockner, K., F. Malard, and J. V. Ward (2000), An extension of the flood pulse concept, *Hydrol. Processes*, *14*, 2861–2883.

U.S. Army Corps of Engineers (1992), Guidelines for risk and uncertainty analysis in water resources planning, Water Resour. Support Cent., Fort Belvoir, Va.

U.S. Army Corps of Engineers (1998), Post-flood assessment for 1983, 1986, 1995, and 1997, Central Valley, California, Sacramento Dist., Sacramento, Calif.

Water Engineering and Technology (1990), Geomorphic analysis of Sacramento River, report, Fort Collins, Colo.

T. Dunne and M. B. Singer, Donald Bren School of Environmental Science and Management, University of California, Santa Barbara, CA 93106, USA. (bliss@bren.ucsb.edu)